e-Journal of Surface Science and Nanotechnology 16 January 2010
e-J. Surf. Sci. Nanotech. Vol. 8 (2010) 27-31 Conference - ACSIN-10 -

Two-Dimensional Electron Transport and Scattering in Bi(111) Surface States*

G. Jnawali,† Th. Wagner,‡ H. Hattab, R. Möller, A. Lorke, and M. Horn-von Hoegen
Faculty of Physics and Center for Nanointegration Duisburg-Essen (CeNIDE), University of Duisburg-Essen, Lotharstr. 1, 47057 Duisburg, Germany
(Received 6 October 2009; Accepted 27 November 2009; Published 16 January 2010)

The Bi(111) surface exhibits a pronounced surface state which acts as dominant transport channel for electric current. We performed *in situ* four-point probe resistance measurements for thin Bi(111) films on Si(001) to study electron scattering effects in this two-dimensional (2D) electron gas. The surface morphology was manipulated by additional deposition of Bi at 80 K. A linear increase of surface resistance was measured at extremely low coverage of less than 1 % of a bilayer (BL) and the slope gradually decreases with coverage up to about 0.5 BL. This behavior was qualitatively explained applying a simple picture of electron scattering at adatoms or small islands during the early stages of growth in Bi(111) homoepitaxy. Beyond 0.5 BL resistance changes periodically showing an antiphase correlation with roughness-induced LEED (00)-spot intensity oscillations, indicating the scattering of electrons at island edges. [DOI: 10.1380/ejssnt.2010.27]

Keywords: Bismuth; Low-energy electron diffraction (LEED); Surface state; 2D electron transport

I. INTRODUCTION

The semimetal bismuth (Bi) is an extensively studied material in solid state physics because of its extreme physical and electronic properties. It has the highest resistivity and Hall coefficients among all metals and exhibits unusual transport phenomena due to very low carrier density and large carrier mobility. The bulk band structure of Bi exhibits tiny hole and electron pockets at the T and L points in the Brillouin zone [1]. This causes the large Fermi wavelength ($\lambda_F \sim 30$ nm) and carrier mean free path of a few microns [2–4]. This leads to the first observation of quantum size effects in thin films in 1966 [5].

In recent years, the interest in epitaxial Bi films has increased dramatically because high quality Bi(111) films have shown intriguing electronic properties near the Fermi level which are defined by strong spin-orbit split surface-state bands [6–8]. From recent photoemission studies [7, 9–11], it was estimated that the carrier density in this surface state is nearly two orders of magnitude higher than in the bulk of the film. Hence the Bi(111) surface may be used as a model system of an ideal 2-dimensional (2D) metal. Recently, Hirahara *et al.* [12] have performed an experiment to directly determine the surface state conductivity via micro-four point probe measurements in ultrathin Bi films. The Bi surface state was destroyed by oxidizing the surface. From the surface conductivity difference before and after the oxidation, an absolute value of the surface state conductivity $\sigma_{ss} = 1.5 \times 10^{-3}\ \Omega^{-1}/\square$ with a carrier density of $n_s \sim 10^{13}$ cm^{-2} was determined which is very large as compared to the corresponding bulk value.

This destruction of the surface state may be considered as the most dramatic manipulation of the 2D conductivity. In order to study scattering effects during 2D electron transport it is desirable to introduce morphological defects in a more subtle manner. In this paper, we will report on a preliminary novel study of the controlled manipulation of the 2D surface state conductivity. Bi adatoms and islands are introduced as scatterers for electrons in the surface state by additional deposition of sub-bilayer coverages of Bi on a smooth Bi(111) base film at 80 K. The simultaneous measurement of surface resistance and surface morphology allows the direct correlation between island size and scattering efficiency. This unique way of measurements allows to investigate the scattering of charge carriers at adatoms or small islands in a 2D electron gas system. A smooth surface could be regained after annealing the film up to 450 K without building of additional roughness.

II. EXPERIMENTAL

The measurements were performed in a UHV chamber with a base pressure of less than 2×10^{-10} mbar. The surface crystal structure and the morphology of the substrate and the film were analyzed by a high resolution SPA-LEED system [13, 14]. The change of the surface morphology during deposition was monitored by the SPA-LEED using a second electron gun in a RHEED-like geometry [14]. A well oriented p-type Si(001) wafer (miscut<0.2°) with a resistivity of 1000 Ω-cm was cut into substrates of $(35\times4\times0.5)$ mm^3 size. High resistivity Si was chosen for the substrate since it behaves like an insulator at low temperature due to the freeze-out of carriers. The electrical resistance was determined *in situ* by macro-four-point probe (4PP) measurements using tungsten disilicide (WSi_2) pads as electrical contacts. The preparation of stable WSi_2 pads on Si and the resistance measurement scheme have been described elsewhere [15].

A clean Si(001) surface was prepared *in situ* by degassing the substrate at 870 K for 6 hours and flash annealing at 1470 K for a few seconds by resistive heating. This process removes the native oxide and results in a (2×1) reconstruction at room temperature and $c(4\times2)$ at 80 K (only on the area where no tungsten was deposited) [16–18], indicating a clean and defect-free surface [19–22]. The sample can be cooled down to 80 K by

*This paper was presented at 10th International Conference on Atomically Controlled Surfaces, Interfaces and Nanostructures (ACSIN-10), Granada Conference Centre, Spain, 21-25 September, 2009.
†Corresponding author: gr.jnawali@uni-due.de
‡Present address: Johannes Kepler University Linz, Institute of Experimental Physics, Altenberger Str. 69, A-4040 Linz, Austria

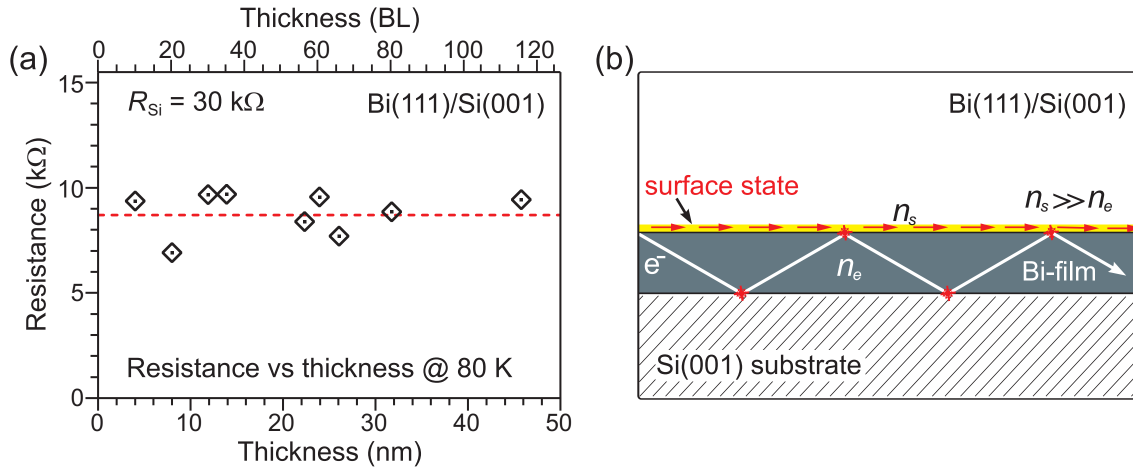

FIG. 1: (a) Resistance of well-annealed Bi(111) films as a function of thickness at 80 K. Dotted line is drawn as a guide to eyes. (b) Schematic view of the electron scattering and transport in Bi films on Si(001). Since at low temperature the surface state electron density in Bi is higher than at the film ($n_s \gg n_e$), the surface provides a dominant channel for charge transport.

using a liquid nitrogen cryostat attached to the sample holder.

Deposition of high-purity Bi (purity: 99.9999 %) was carried out by thermal evaporation from a directly heated ceramic crucible mounted in a water-cooled copper shroud. During deposition, the residual pressure was better than 4×10^{-10} mbar. A high quality Bi(111) base film was prepared on a Si(001) substrate following a recipe resulting in extremely smooth Bi(111) surfaces with large terraces [23]. A deposition rate of 0.6 bilayer/minute (BL/min) [1 BL=1.14×10^{15} atoms/cm^2 with a thickness of 0.394 nm] was maintained during each deposition process. The deposition rate was monitored by a quartz crystal microbalance. A precise thickness calibration was obtained from BL intensity oscillations of the LEED (00)-spot intensity with coverage during Bi deposition on the Bi(111) base film [24].

III. RESULTS AND DISCUSSION

A. Smooth Bi(111) base films at 80 K

The electrical transport measurements were performed at 80 K on various smooth Bi(111) base films prepared as described above. Prior to each measurement the morphology of the films was analyzed by SPA-LEED to confirm that all the films have a smooth surface. Figure 1(a) shows the resistance of these Bi films from t = 2 nm to 50 nm thickness. The data clearly show a constant resistance within the range of reasonable experimental errors. The resistance of the Si substrate at 80 K is R_{Si} = 30 kΩ, which is three times higher than the Bi base film resistance and therefore may be neglected. During the course of the experiment the contribution of the Si substrate to the current transport stays constant and is independent of the film preparation. It may therefore be considered as a constant resistance parallel to the Bi film resistance.

Obviously the constant resistance up to 50 nm thickness could not be explained by bulk-like transport expecting a $1/t$ (t=film thickness) behavior or by thin film transport with additional surface scattering according to the Fuchs-Sondheimer model [25, 26] expecting a $1/t^2$ behavior. The constant resistance is only explained if the surface offers the dominant channel for electrical transport which is provided by a metallic surface state as previously detected by photoemission spectroscopy measurements [8]. We assume the situation as sketched in Fig. 1(b). Since the surface electron density (n_s) is much higher than the electron density in the bulk of the film (n_e) [12], the current mainly flows through the surface state. The contribution of the bulk of the Bi film to the current transport is negligible because the carrier density is of the order of only 10^{17} cm^{-3}.

B. Bi on Bi(111) base film at 80 K

In a next step additional Bi was evaporated on a 9 nm Bi(111) base film at 80 K. We have chosen such a small thickness because any contribution to the conductivity from the bulk of the Bi film will be minimized. The solid red line in Fig. 2(a) shows the relative change of the film resistance as a function of additional coverage. The relative change of the resistance was calculated via $\triangle R/R_0 = (R(t) - R_0)/R_0$, where $R(t)$ is the measured resistance with increasing thickness t and R_0 is the initial resistance of the base film. In the following, the overall resistance behavior will be explained by dividing it into a (1) low coverage (< 0.5 BL) and (2) high coverage regime (> 0.5 BL).

1. *Low coverage regime (<0.5 BL)*

The resistance increases drastically at the early stages of growth and the increase slightly slows down until 0.5 BL (Fig. 3). Within half a BL coverage, the resistance increases nearly 17 % of the initial base film resistance. Within the additional 0.5 BL coverage, the measured relative resistance can be separated into three different regimes, i.e., 0-1 %, 1-10 %, and 10-50 % of a bilayer, considering the change of slope as a function of thickness. A close inspection indicates that the curve could be fit-

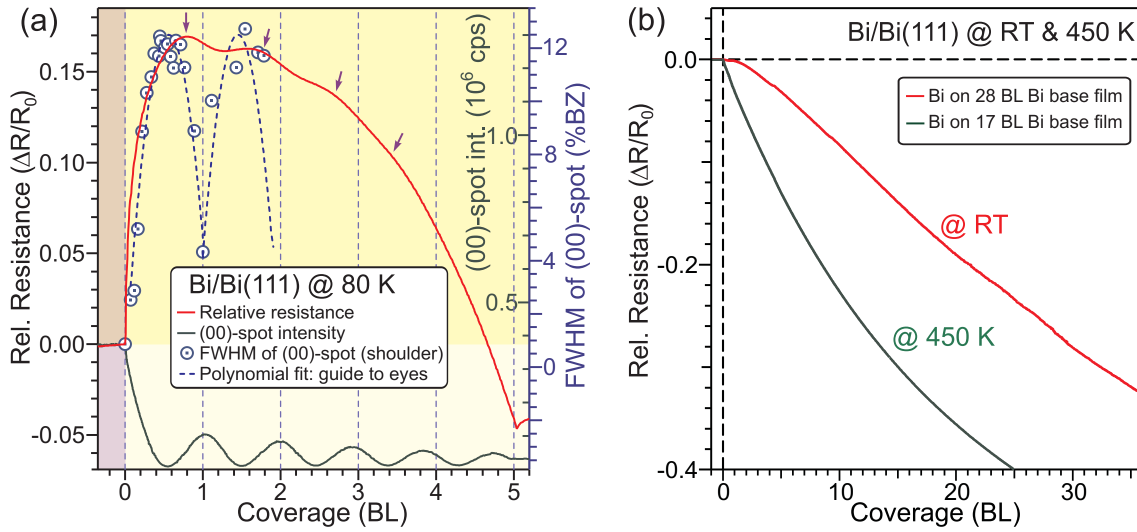

FIG. 2: (a) Relative change of resistance (red curve) and the LEED (00)-spot intensity (green curve) during additional deposition of Bi on Bi(111) base films at 80 K. The LEED (00)-spot intensity oscillation reflects a 2D bilayer-by-bilayer growth mode. Periodic change of the (00)-spot width (the blue symbol) shows a variation of island density during deposition. Such a periodic change of surface morphology also induces an oscillation of the resistance. The oscillation amplitude could be observed up to four maxima (blue arrows). (b) Relative change of resistance with coverage during additional deposition of Bi on Bi(111) base films at RT and 450 K. The resistance immediately decreases with coverage exhibiting a bulk-like behavior.

ted with linear function ($\propto \Theta$) at extremely low coverage regime and square of the cubic root function ($\propto \Theta^{2/3}$) up to 10 % of a BL coverage (Fig. 3). Beyond 10 % of a BL, the slope decreases further with coverage up to 0.5 BL.

The first linear regime, up to 1 % of a BL, could be easily explained in the context of early stages of growth in Bi(111) homoepitaxy. During the additional deposition Bi atoms are randomly adsorbed on commensurate sites of Bi(111) surface. Due to the low deposition temperature these adatoms can hardly diffuse across the surface and therefore statistically distributed as isolated point defects. Since the adatom density is too low for the nucleation of islands, each individual adatom acts like a single scatterer for conduction electrons in the surface state with a scattering cross-section of an individual Bi adatom Ω_1. As a consequence the resistance increases linearly with the adatom density n_1 or Bi coverage Θ. Hence:

$$\triangle R/R_0 \propto (\Omega_1 \cdot n_1) \propto \Theta. \qquad (1)$$

In the second regime between 1−10 % of a bilayer coverage the slope of $\triangle R/R_0$ continuously decreases. With increasing coverage the adatom density becomes high enough for the nucleation of stable 2D-islands. The increasing number of islands must act as scattering centers for the 2D transport in the surface state. In the following we apply a simple Drude-type approach of electron scattering to explain the observed behavior. The scattering probability of the electrons in the surface state is assumed to be proportional to the density of islands multiplied by the island perimeter as scattering cross section. Thus for a higher density of islands at higher coverage a lower value of scattering mean free path l_x would be expected.

In a STM study [27] of the nucleation regime of Bi on Bi(111) it was shown that the island density n_x increases with the cubic root of Bi coverage $n_x \sim \Theta^{1/3}$. Thus the average island size increases as $A_x \sim \Theta/n_x \sim \Theta^{2/3}$ and the average perimeter as $p_x \sim A_x^{1/2} \sim \Theta^{1/3}$. With the mean free path of the electrons $l_x \sim 1/n_x$ and a scattering cross-section proportional to p_x we expect a change of resistance

$$\triangle R/R_0 \ \propto \ \frac{p_x}{l_x} \sim \Theta^{2/3}. \qquad (2)$$

At least up to 10 % of a BL, the 2/3 dependence matches the data well (solid green line in Fig. 3). Beyond 10 % of a BL, the slope of the resistance gradually decreases and levels off at 0.5 BL. The decrease of the slope might be caused by the opening of an additional path of electron transport through the surface state in 2D islands as the island size becomes larger than the surface state electron mean free path l_{el}, i.e., 5 nm in the case of Bi(111) [12]. This trend continues until the coalescence regime, since island size increases with coverage, and therefore we see an increased contribution of electron transport by a gradual decrease of resistance slope (Fig. 3).

2. *High coverage regime (>0.5 BL)*

Beyond 0.5 BL the resistance shows weak oscillations before it finally starts to decrease monotonously. The period of the oscillation matches with the period of the LEED (00)-spot intensity oscillations. The maxima, however, are in anti-phase correlation as indicated by the arrows in Fig. 2(a), suggesting that the periodic change of the surface step density causes the oscillation in the relative resistance.

If growth occurs in a bilayer-by-bilayer mode, the surface roughness or step density oscillates from a minimum at a complete layer to a maximum at a half integer order of coverage. At the lowest roughness, i.e., the integer layer coverage, the scattering probability is minimal due to the minimal surface step density. This results in the minimal surface resistance. At the highest roughness, i.e.,

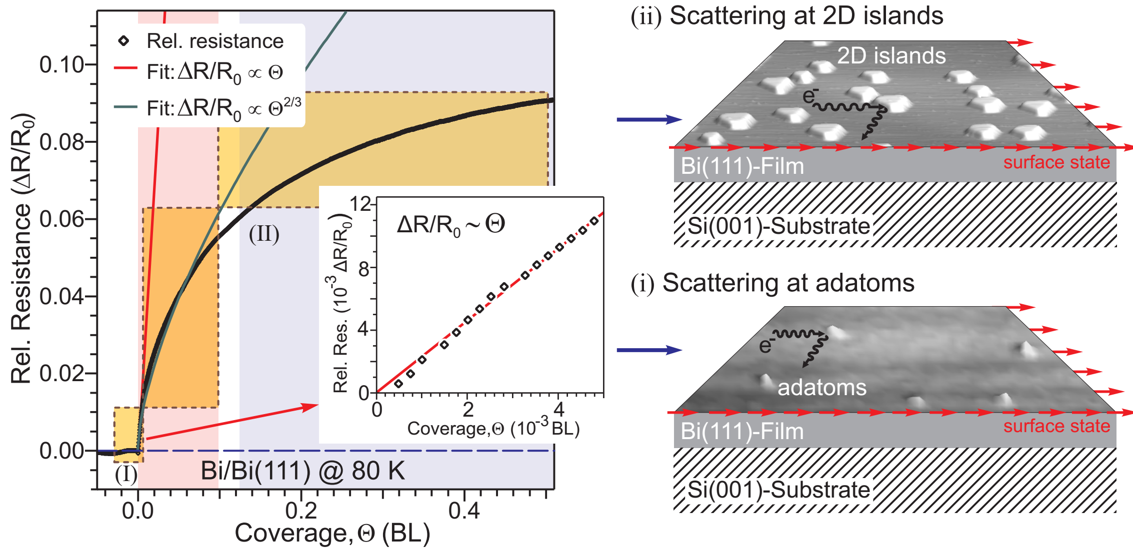

FIG. 3: Relative change of resistance during deposition of Bi on a 9 nm Bi(111) film at 80 K. The solid red line shows the linear fit of the measured data up to the 1 % of a BL. Inset shows the close-up view of the linear plot. To the right, sketches of the underlying scattering mechanisms are shown: (i) carrier scattering at adatoms (white protrusions), which causes linear increase of the resistance, and (ii) carrier scattering at 2D islands (white area), which causes decrease of the slope.

the half integer layer coverage, the scattering probability is highest due to the maximal step density at surface and results in the maximal surface resistance. Such a periodic variation of the surface step density modulates the resistance and shows up as an oscillation.

The periodic change of surface morphology was additionally investigated through the precise roughness analysis during deposition via recording the full width at half maximum (FWHM) of the diffuse intensity of the (00)-spot profiles, which is inversely proportional to the lateral size of the islands [14]. The blue circles (scale on the right y-axis) in Fig. 2(a) show the FWHM of the diffuse intensity, with a maximum at the minimum of the LEED intensity peak and vice versa. Thus the periodic BL variation of the step density explains the resistivity oscillations.

Despite a constant period (1 BL) of all three oscillations, i.e., resistance, FWHM and the (00)-peak intensity, small change of the peak positions of the maximum or the minimum for all oscillations are observed. This behavior reflects the slight variation of the layer distribution during growth. That means the second layer starts before the completion of the first layer as growth proceeds. Such a variation of layer distribution slightly shifts the peak position towards higher coverage in the resistance curve. In the course of the deposition, the oscillation amplitudes are strongly damped and finally disappear at higher coverage, caused by the gradual increase of surface roughness with coverage, as indicated by the reduced amplitudes of the LEED (00)-spot intensity peaks in Fig. 2(a).

Finally, at higher coverage, the resistance decreases rapidly and monotonously, showing a typical thickness-dependent resistance behavior as in metallic thin films [28]. This seems like a paradox in a sense that almost all surface states may be destroyed due to the increasing surface roughness and the resistance is still decreasing monotonously with coverage. This is a strong hint that only those excess carriers which are spilled out of the surface states to the conduction band may take part in the electrical conduction. However, this is yet to be confirmed by systematic experimental investigation.

C. Bi on Bi(111) base film at higher temperatures

In contrast to the measurements at 80 K, the resistance decreases immediately for deposition of Bi on smooth Bi(111) base films at room temperature (see Fig. 2(b)). This is due to two effects: the carrier concentration increases with temperature in Bi films and results in a dominating bulk conductivity of the films [12]. In addition the growth mode changes from bilayer-by-bilayer to step-flow mode as the deposition temperature is increased [24].

As in the case of metallic films on semiconductor such as Ag films on Si [28], obviously, the films have shown a typical thickness-dependent $1/t^2$ behavior following a classical electron scattering model of Fuchs-Sondheimer [25, 26]. The decrease of the resistance occurs faster at 450 K than at RT, which is caused by the increased probability of specular reflection p due to improved growth at 450 K. At RT, growth proceeds in a quasi step-flow mode [24] and a slight buildup of surface roughness always occurs, which contributes to the resistance by reducing the value of p. In contrast, at 450 K, growth proceeds in a perfect step-flow mode (i.e., constant step density with coverage) and therefore additional contribution to the resistance decreases drastically due to nearly 100 % probability of specular reflection at surface boundary, i.e., the value of p close to 1. This causes the decrease of the resistance even faster at 450 K (Fig. 2(b)).

IV. CONCLUSION

We have shown that electron transport in Bi films at 80 K is dominated by the transport through the surface

state. This was used as a model system to study the electron scattering effects in a 2D electron gas system during additional deposition of Bi at 80 K. We observed clear evidence of electron scattering at single adatoms and the scattering at island edges. A simple picture of electron scattering and the early stage homoepitaxial growth of Bi(111) were applied to explain the resistance behavior.

Acknowledgments

Financial support from the Deutsche Forschungsgemeinschaft through SFB 616 "Energy Dissipation at Surfaces" is gratefully acknowledged.

[1] Ph. Hofmann, Prog. Surf. Sci. **81**, 191 (2006).
[2] D. H. Reneker, Phys. Rev. Lett. **1**, 440 (1958).
[3] W. S. Boyle and G. E. Smith, Prog. Semicond. **7**, 1 (1963).
[4] N. Garcia, Y. H. Kao, and M. Strongin, Phys. Rev. B **5**, 2029 (1972).
[5] Yu. F. Ogrin, V. N. Lutskii, and M. I. Elinson, JETP Lett. **3**, 71 (1966).
[6] Yu. M. Koroteev, G. Bihlmayer, J. E. Gayone, E.V. Chulkov, S. Blügel, P. M. Echenique, and Ph. Hofmann, Phys. Rev. Lett. **93**, 046403 (2004).
[7] T. Hirahara, T. Nagao, I. Matsuda, G. Bihlmayer, E. V. Chulkov, Yu. M. Koroteev, P. M. Echenique, M. Saito, and S. Hasegawa, Phys. Rev. Lett. **97**, 146803 (2006).
[8] T. Hirahara, K. Miyamoto, I. Matsuda, T. Kadono, A. Kimura, T. Nagao, G. Bihlmayer, E. V. Chulkov, S. Qiao, K. Shimada, H. Namatame, M. Taniguchi, and S. Hasegawa, Phys. Rev. B **76**, 153305 (2007).
[9] M. Hengsberger, P. Segovia, M. Garnier, D. Purdie, and Y. Baer, Eur. Phys. J. B **17**, 603 (2000).
[10] C. R. Ast and H. Höchst, Phys. Rev. Lett. **87**, 177602 (2001).
[11] C. R. Ast and H. Höchst, Phys. Rev. B **67**, 113102 (2003).
[12] T. Hirahara, I. Matsuda, S. Yamazaki, N. Miyata, S. Hasegawa, and T. Nagao, Appl. Phys. Lett. **91**, 202106 (2007).
[13] U. Scheithauer, G. Meyer, and M. Henzler, Surf. Sci. **178**, 441 (1986).
[14] M. Horn-von Hoegen, Z. Kristallogr. **214**, 591 & 684 (1999).
[15] G. Jnawali, F.-J. Meyer zu Heringdorf, D. Wall, S. Sindermann, and M. Horn-von Hoegen, J. Vac. Sci. Technol. B **27**, 180 (2009).
[16] D. J. Chadi, Phys. Rev. Lett. **43**, 43 (1979).
[17] T. Tabaka, T. Aruga, and Y. Murata, Surf. Sci. **179**, L63 (1987).
[18] R. A. Wolkow, Phys. Rev. Lett. **68**, 2636 (1992).
[19] R. M. Tromp, R. J. Hamers, and J. E. Demuth, Phys. Rev. Lett. **55**, 1303 (1985).
[20] M. Kubota and Y. Murata, Phys. Rev. B **49**, 4810 (1994).
[21] T. Aruga and Y. Murata, Phys. Rev. B **34**, 5654 (1986).
[22] S. Matsuura, T. Hitosugi, S. Heike, A. Kida, Y. Suwa, T. Onogi, S. Watanabe, K. Kitazawa, and T. Hashizume, Jpn. J. Appl. Phys. **39**, 4518 (2000).
[23] G. Jnawali, H. Hattab, B. Krenzer, and M. Horn-von Hoegen, Phys. Rev. B **74**, 195340 (2006).
[24] G. Jnawali, H. Hattab, C. A. Bobisch, A. Bernhart, E. Zubkov, R. Möller, and M. Horn-von Hoegen, Phys. Rev. B **78**, 035321 (2008).
[25] K. Fuchs, Proc. Camb. Phil. Soc. **34**, 100 (1938).
[26] E. H. Sondheimer, Adv. Phys. **1**, 1 (1952).
[27] G. Jnawali, Th. Wagner, H. Hattab, R. Möller, and M. Horn-von Hoegen, Phys. Rev. B **79**, 193306 (2009).
[28] D. Schumacher and D. Stark, Surf. Sci. **123**, 384 (1982).